α-Al_2O_3 Improves the Properties of Gel Polyacrylonitrile Nanocomposite Electrolytes Used as Electrolyte Materials in Rechargeable Lithium Batteries

Jiunn-Jer Hwang,[1] Hsueh-Hsin Peng,[2] Jui-Ming Yeh[3]

[1]*Department of Chemical Engineering, Army Academy, Chung-Li, Taiwan, Republic of China*
[2]*Department of Chemical and Materials Engineering, Vanung University, Chung-Li, Taiwan, Republic of China*
[3]*Department of Chemistry, Center for Nanotechnology at CYCU and R&D Center for Membrane Technology, Chung-Yuan Christian University, Chung-Li, Taiwan, Republic of China*

Received 29 April 2010; accepted 29 August 2010
DOI 10.1002/app.33311
Published online 8 December 2010 in Wiley Online Library (wileyonlinelibrary.com).

ABSTRACT: In this investigation, a series of gel polyacrylonitrile (PAN)/α-Al_2O_3 nanocomposite electrolyte materials that incorporate various fractions of PAN, α-Al_2O_3 inorganic powders, propylene carbonate and ethylene carbonate as cosolvents, and $LiClO_4$ were prepared. X-ray diffraction revealed that the gel nanocomposite electrolyte materials contained amorphous PAN in which was uniformly dispersed α-Al_2O_3. The gel PAN/α-Al_2O_3 nanocomposite electrolytes had lower glass-transition temperatures (as determined by dynamic mechanical analysis) and higher conductivity than a similar electrolyte prepared in the absence of α-Al_2O_3. The conductivity of the PAN/α-Al_2O_3 nanocomposite films was inversely proportional to the size of the α-Al_2O_3 particles and directly proportional to (I) the amount of α-Al_2O_3 (up to 7 wt %), (II) the *F* value [$LiClO_4/CH_2CH(CN)$ ratio], and (III) the amount of plasticizer (propylene carbonate/ethylene carbonate = 1 : 1). Cyclic voltammetry revealed that adding α-Al_2O_3 significantly increased the electrochemical stability of the composite electrolyte system. A rechargeable lithium battery prepared using this gel nanocomposite electrolyte system exhibited good cyclability and a stable capacity. The coulombic efficiency for the recharge/discharge process was approximately 75%, even after 100 cycles. © 2010 Wiley Periodicals, Inc. J Appl Polym Sci 120: 2041–2047, 2011

Key words: gel electrolyte; aluminum oxide; polynitrile; rechargeable lithium battery; conductivity

INTRODUCTION

Numerous modern electronic appliances and related products are preferably wireless, mobile, versatile, lightweight, thin, and compact. Because batteries are crucial components of such devices, they must meet certain standards of reliability, weight, size, shape, and environmental impact. Lithium polymer secondary batteries were developed to satisfy these requirements.[1–4] The polymer electrolyte materials in a lithium polymer secondary battery system have two functions; as an electrolyte and as a separator between the anode and the cathode. Their ionic conductivities, dimensions, and electrochemical stabilities must fulfill certain requirements.[5,6]

Gel polymer electrolytes (GPEs), which comprise an electrolyte solution and a host polymer, have better conductivity and dimensional stability than solid polymer electrolytes,[7–10] and they are more stable against thermal and mechanical stress, especially in the packaging procedure. Several polymers have been used as basic materials in GPEs. They include poly(vinyl chloride),[11] poly(vinylidene fluoride),[12] poly(vinylidene fluoride-*co*-hexafluoropropylene),[13–15] polyacrylonitrile (PAN),[16,17] poly(vinyl pyrrolidone),[18] and poly(ethylene glycol diarylate).[19] Additionally, gel films based on poly(vinylidene fluoride), poly(methyl methacrylate), and PAN have been used as polymer electrolytes in rechargeable lithium batteries that provide output voltages of 3 V and coulombic efficiencies of 90–100%.[20–25]

One of the most promising ways to improve the electrochemical performance and thermal stability of polymer electrolytes is to form a composite electrolyte by adding inorganic (ceramic) powder or organophilic montmorillonite clays to such an electrolyte, retaining an ionic conductivity of 10^{-3} to 10^{-6} S cm^{-1}.[26–34] These composite electrolytes are associated with considerably better capacity and efficiency of circulation in lithium polymer secondary batteries,[35,36] while inhibiting the formation of passivation films between the electrolyte and the electrodes during charging.[37–39]

Correspondence to: J.-J. Hwang (jiunnjer1@hotmail.com).
Contract grant sponsor: National Science Council of the Republic of China, Taiwan; contract grant number: NSC93-2216-E-238-001.

This study describes the preparation of a series of gel PAN nanocomposite electrolytes that incorporate α-Al_2O_3 nanopowder, and elucidates the effects of their dispersion stabilities, ionic conductivities, glass-transition temperatures (T_g), electrochemical stabilities, and cyclic recharging on the performance of lithium PAN/α-Al_2O_3 secondary batteries that use them.

EXPERIMENTAL

Materials

PAN (M_w 150,000) was purchased from Polysciences (Warrington, PA). Lithium perchlorate ($LiClO_4$) was obtained from Fluka Synthesis (St. Louis, MO). Ethylene carbonate (EC) was purchased from Acros Organics (Geel, Belgium). Propylene carbonate (PC) was obtained from Lancaster Organics (Lancaster, MA). Acetone was purchased from Merck Chemicals Co. (Nottingham, UK). α-Al_2O_3 (50, 100 nm) was purchased from Grace Derwey Co. (Taipei, Taiwan). α-Al_2O_3 (80 nm) was purchased from Desunnano Co. (Taipei, Taiwan). PAN was dried in a vacuum for 24 h at 65°C before use. $LiClO_4$ and α-Al_2O_3 were dried in a vacuum for 24 h at 130°C before use. All other reagents and solvents were used as received.

Preparation of gel PAN/α-Al_2O_3 nanocomposite electrolytes

α-Al_2O_3 (1, 3, 5, 7, or 9 wt %) and $LiClO_4$ {F = [$LiClO_4$/$CH_2CH(CN)$] = 0.3, 0.4, 0.5, or 0.6, where F represents the molar ratio of salt to a PAN repeat unit} were separately mixed with PC/EC cosolvents (1 : 1, v/v) under ultrasonication at room temperature. PAN powder (0.5 g) was then dissolved into a PC/EC cosolvent (1 : 1, v/v) with stirring for 1 h at 60°C. The $LiClO_4$ solution was added to the transparent polymer solution and stirred for 1 h at room temperature. The suspension of α-Al_2O_3 was then added, and the mixture was stirred for 24 h at room temperature. Gel PAN electrolyte films were prepared by casting the solution onto a glass plate and then partially removing the solvent in an oven at 100°C. The thickness of the films varied between 0.10 and 0.12 mm. Table I presents the relationship between GPE sample and code. The resulting freestanding films of gel PAN/α-Al_2O_3 nanocomposite electrolytes, which had solvent contents of 25–55 wt %, were stored in a glove box.

Characterization

Wide-angle X-ray diffraction (XRD) analysis of the samples was carried out using a Rigaku D/MAX-3C OD-2988N X-ray diffractometer (The Woodlands, TX) that was equipped with a Cu target and an Ni filter and operated at a scanning rate of 10° min^{-1}. Dynamic mechanical analysis (DMA) measurements of the freestanding films of the gel PAN/α-Al_2O_3 nanocomposite electrolytes were made using a DMA Q800 apparatus (New Castle, DE). Ionic conductivities were measured at 30°C in a vacuum chamber using an HP4192A impedance analyzer (Agilent, Santa Clara, CA) that was operated at frequencies from 0.1 Hz to 1 MHz. The GPE films were sandwiched between two Au electrodes. The ionic conductivity was calculated from the impedance of the cell. The lithium plating/stripping process was evaluated from the cyclic voltammetry (CV) data that were obtained from a three-electrode cell, consisting of a stainless-steel working substrate, a lithium counter electrode, and a lithium reference electrode. The CV curves were obtained at room temperature using a PGSTAT30 potentiostat/galvanostat (Eco Chemie B.V., the Netherlands) that was linked to a personal computer. The discharge/recharge process of the coin cell (thickness = 3.2 mm and diameter = 20 mm) was measured at room temperature using an Arbin BT2000 Cycler (College Station, TX) at the 1°C rate with voltage cut-off limits of 2.7 and 3.8 V. All coin cells were assembled by sandwiching the polymer nanocomposite electrolyte between the lithium anode and the $LiCoO_2$ cathode in a glove box that was filled with gaseous argon.

TABLE I
Different Component Ratio Matrix for Code of Gel PAN Nanocomposite Electrolytes

GPEs sample code	(F) F-value	(A) α-Al_2O_3 (wt %)	(P) Nanoparticle size (nm)
F6A0	0.6	0	–
F3A5P50	0.3	5	50
F3A5P80	0.3	5	80
F3A5P100	0.3	5	100
F6A1P50	0.6	1	50
F6A3P50	0.6	3	50
F6A5P50	0.6	5	50
F6A7P50	0.6	7	50

RESULT AND DISCUSSION

Gel PAN/α-Al_2O_3 nanocomposite electrolytes

The XRD patterns of $LiClO_4$, α-Al_2O_3, and PAN (Fig. 1) demonstrate that $LiClO_4$ and α-Al_2O_3 were crystalline compounds, whereas PAN, which yielded only a single diffraction peak at $2\theta = 16°$, was a weakly crystalline polymer.

Homogeneous solutions were obtained after a solution of PAN and $LiClO_4$ ($F = 0.6$) was mixed with various amounts of 50 nm α-Al_2O_3 solutions (0, 1, 3,

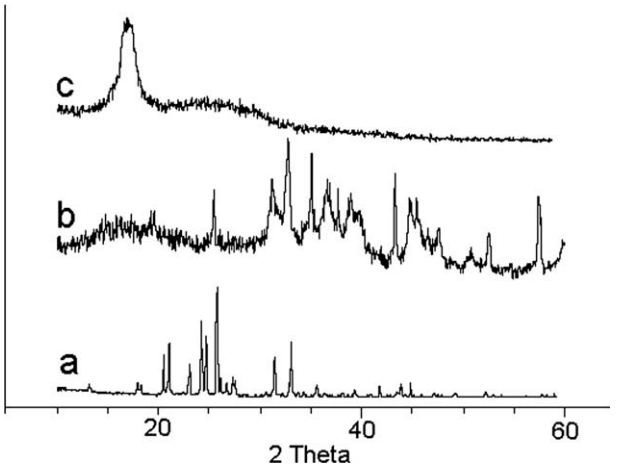

Figure 1 XRD patterns of (a) $LiClO_4$, (b) α-Al_2O_3, and (c) PAN.

5, 7, or 9 wt %). Casting these solutions on a glass plate yielded films of gel PAN/α-Al_2O_3 nanocomposite electrolytes. The XRD patterns of these films (Fig. 2) include none of the diffraction peaks that were observed from pure PAN, $LiClO_4$, or α-Al_2O_3, suggesting that the order of the crystalline domains of PAN had been destroyed and that amorphous PAN had formed. They also indicate that $LiClO_4$ and α-Al_2O_3 had dissolved completely in the polymer electrolyte, causing these materials to be mostly amorphous states. Independently of the α-Al_2O_3 content, the XRD patterns of the films were very similar, including only a single broad diffraction peak at $2\theta = 7^\circ$, which was associated with the amorphous phase of PAN.

DMA was used to determine the maximum loss tangents, tan δ, of the gel PAN nanocomposite electrolytes F6A0, F6A3P50, and F6A7P50, which were −9.78, −22.65, and −20.52°C, respectively (Fig. 3). The significant declines in tan δ on the addition of α-Al_2O_3 correspond to decrease in T_g and the softening points of the gel PAN nanocomposite electrolytes. This phenomenon increases the number of degrees of freedom of the polymer chains and promotes the migration of the ions.

Ionic conductivity

The conductivity of the gel PAN nanocomposite electrolytes is consistent with the equation $\sigma = L/(A \times R_b)$, where σ is the specific conductivity; R_b is the bulk resistance (determined from AC impedance); L is the thickness of the film, and A is the surface area of the electrode. Table II presents the ionic conductivity of the GPEs nanocomposite. Figure 4 shows that adding α-Al_2O_3 power increased the conductivity of the gel PAN electrolyte. Previous investigations have suggested that the migration of

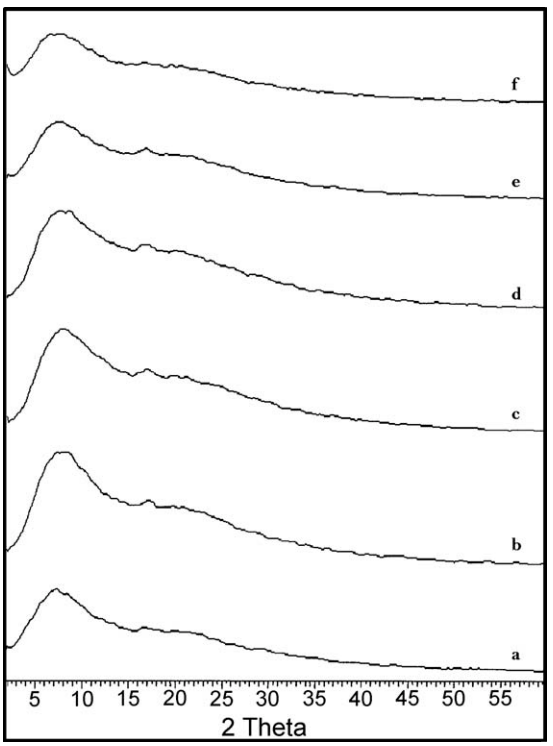

Figure 2 XRD patterns obtained after adding different amounts of α-Al_2O_3 into GPE: (a) F6A0, (b) F6A1P50, (c) F6A3P50, (d) F6A5P50, (e) F6A7P50, and (f) F6A9P50.

lithium ions in polymer electrolytes is activated at temperatures close to T_g because of the increased flexibility of the polymer chain.[40,41] Based on the DMA data, the gel PAN electrolytes that incorporate α-Al_2O_3 powder had lower values of T_g and, therefore, higher conductivities. Smaller particles in α-Al_2O_3 powder are also associated with greater conductivity of the GPEs;[42] these results are consistent with previous findings. We posit that the Lewis-

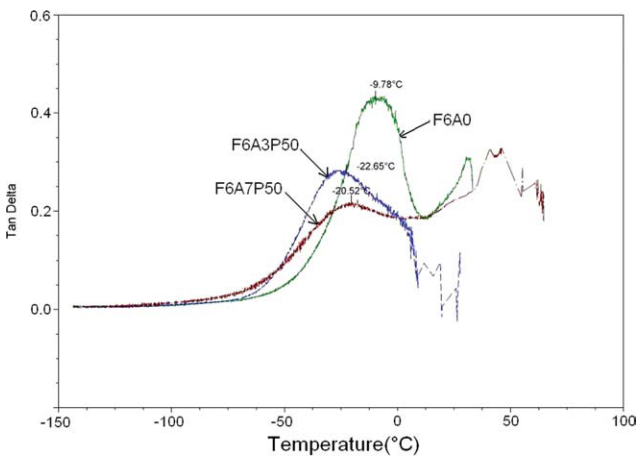

Figure 3 DMA traces of gel PAN nanocomposite electrolytes containing various amounts of 50 nm α-Al_2O_3. [Color figure can be viewed in the online issue, which is available at wileyonlinelibrary.com.]

TABLE II
The Conductivity (σ) of GPEs Nanocomposites by R_b ($-Z'$, $-Z''$ of Impedance Spectrum), L (Thickness of Films), and A (Surface Area of the Specimen: 1.2272 cm^2)

GPEs nanocomposites	R_b (Ω)[a]	L (mm)	σ (S cm^{-1})[a] ($\times 10^{-4}$)
F3A0	30.70	0.110	2.92
F3A7P100	28.37	0.110	3.16
F3A7P80	21.13	0.105	4.05
F3A7P50	20.94	0.110	4.28
F4A0	16.56	0.100	4.92
F4A7P100	15.17	0.100	5.37
F4A7P80	15.09	0.105	5.67
F4A7P50	14.53	0.105	5.89
F5A0	15.92	0.110	5.63
F5A7P100	14.83	0.105	5.77
F5A7P80	14.45	0.105	5.92
F5A7P50	13.18	0.105	6.49
F6A0	15.12	0.110	5.93
F6A7P100	12.38	0.100	6.58
F6A7P80	13.20	0.110	6.79
F6A7P50	11.44	0.105	7.48
F6A1P50	14.55	0.110	6.16
F6A3P50	13.79	0.110	6.50
F6A5P50	13.34	0.110	6.72
F6A9P50	15.35	0.120	6.37

The amount of the co-solvent was 50 wt %.
[a] At 30°C.

acidic surface of α-Al_2O_3 interacted with PAN, weakening the interactions between the lithium ions and the nitrile group of PAN.[43] The presence of α-Al_2O_3 also reduced the attraction between the lithium ions and the perchlorate ions, increasing the number of degrees of freedom and thereby accelerating the transfer of lithium ions. Because smaller α-Al_2O_3 particles are associated with a larger total surface area and provide more Lewis acid centers,

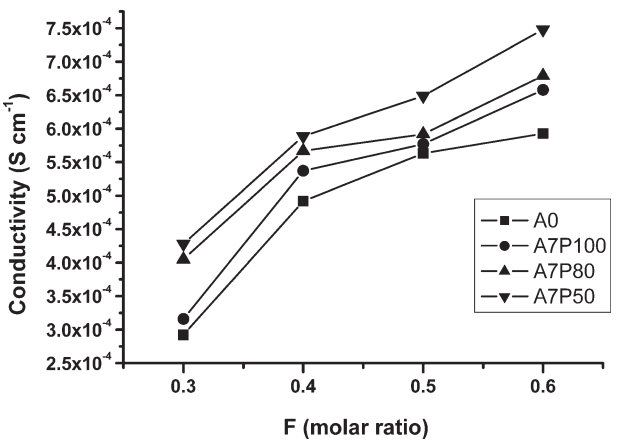

Figure 4 Plot of conductivity with respect to $LiClO_4$ content (F value) for gel PAN nanocomposite electrolytes in the absence and presence of α-Al_2O_3 (7 wt %) of various particle sizes at 30°C. The amount of the cosolvent was 50 wt %.

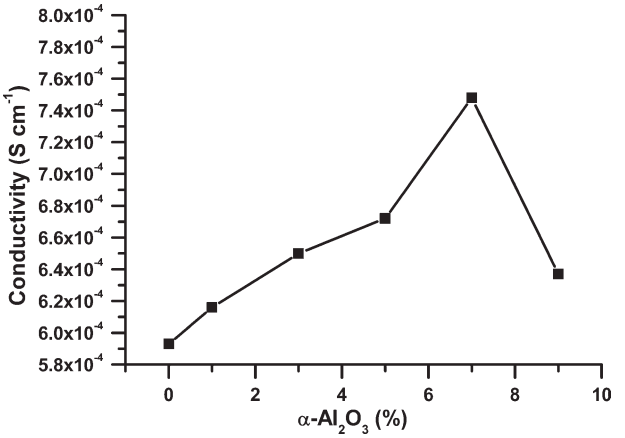

Figure 5 Plot of conductivity at 30°C with respect to the content of 50-nm α-Al_2O_3 for gel PAN nanocomposite electrolytes ($F = 0.6$) containing 50 wt % cosolvent.

they are associated with a higher number of free lithium ions available to act as electrical carriers and, therefore, higher conductivity. The conductivity was also related to the $LiClO_4$ concentration; Figure 4 reveals that the conductivity of the gel PAN electrolyte increased with F.

Although the incorporation of α-Al_2O_3 increased the conductivity of the GPEs (by weakening the interactions between lithium ions and perchlorate ions and between lithium ions and nitrile groups), this advantageous effect was strongest at a particular amount added, because of poor dispersion and aggregation. Figure 5 shows that the conductivity of the gel PAN electrolyte with a thickness of 0.10 mm and a solvent content of 50% increased to 7.48 $\times$ 10^{-4} S cm^{-1} as the α-Al_2O_3 content increased to 7 wt %; further increases in the α-Al_2O_3 content greatly reduced conductivity.

Next, the effects of the plasticizer content and the thickness of the GPE film on the conductivity of the resulting polymer electrolytes are examined. Generally, increasing the amount of solvent in a film reduces its mechanical strength and inhibits film formation. Figure 6 demonstrates that increasing the amount of plasticizer (PC/EC = 1 : 1) increased the conductivity. Because this plasticizer, which has high polarity and dielectric constant, dissolved $LiClO_4$ effectively, it dispersed the lithium ions into the polymer electrolyte system to a degree that was proportional to the amount present. Moreover, the viscosity of the system declined as the amount of cosolvents increased, promoting the transfer of ions in the polymer electrolyte.

Electrochemical stability

A suitable GPE for use in a lithium polymer secondary battery must have not only high conductivity but also good electrochemical stability.

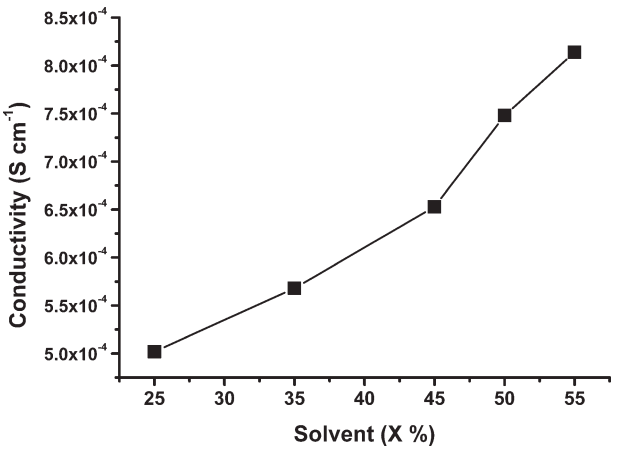

Figure 6 Plot of conductivity at 30°C with respect to plasticizer content (PC/EC = 1 : 1) for the gel PAN nanocomposite electrolyte F6A7P5.

Therefore, the gel PAN/α-Al_2O_3 nanocomposite electrolyte films with superior conductivity were subjected to electrochemical testing. In a half-cell, Li/GPE/Li was used as both the counter electrode and the reference electrode, and the working electrode was a piece of platinum. This assembly was placed in a storage tank that had been filled with argon gas, and CV was used to examine the cyclic oxidation/reduction effect of lithium ions. All of the electrolytes that were prepared for this test contained 50 wt % cosolvent and had a film thickness of about 0.1 mm. The gel PAN/α-Al_2O_3 nanocomposite electrolyte films had an anodic decomposition potential of approximately 4.2 V. Figures 7 and 8 demonstrate that the number of cycles of the gel PAN nanocomposite electrolyte F6A7P50, which contained 7 wt % of the 50 nm α-Al_2O_3 powder with an *F* value of $LiClO_4$ of 0.6, considerably exceeded that of F3A5P50, which contained 5 wt %

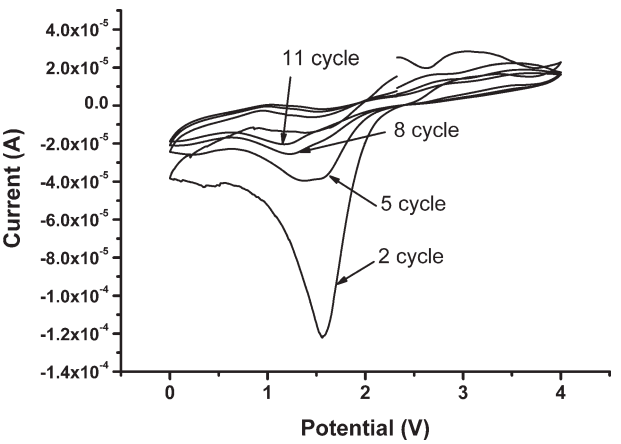

Figure 7 Cyclic voltammograms of the Li/GPE(F3A5P50)/Li cell. Lithium metal was used for counter electrode and reference electrode (scan rate: 1 mV s^{-1}).

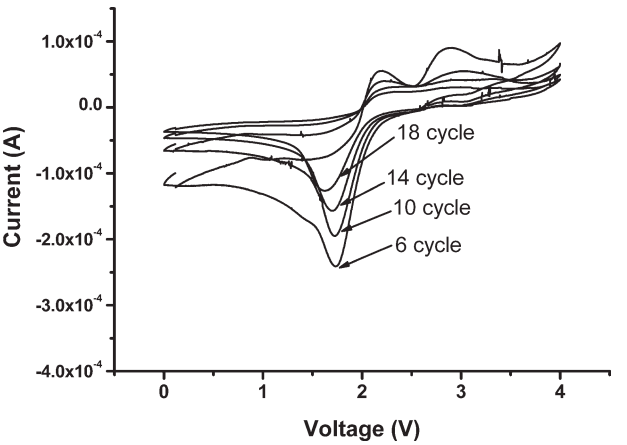

Figure 8 Cyclic voltammograms of the Li/GPE (F6A7P50)/Li cell. Lithium metal was used for counter electrode and reference electrode (scan rate: 1 mV s^{-1}).

of the 50 nm α-Al_2O_3 and had an *F* value of $LiClO_4$ of 0.3 : F6A7P50 exhibited less a decline in the peak current on repeated cycling. Increasing the amount of α-Al_2O_3 increased the flexibility of the PAN, reduced the attraction between lithium ions and the nitrile groups of PAN, reduced the degree of association between the lithium and perchlorate ions, and reduced the degree of passive film formation. Furthermore, a larger dissociated $LiClO_4$ content was associated with a higher effective lithium ion content and a greater reversibility of the loss and gaining of electrons by lithium. Therefore, because the electrochemical stability of the gel PAN/α-Al_2O_3 nanocomposite electrolytes was moderate for particular compositions, their cyclic recharging in lithium polymer secondary batteries was tested.

Performance of Li/Gel PAN/α-Al_2O_3 electrolyte/composite cells

To test cyclability, coin cells that contained a $LiCoO_2$ material that was based on an aluminum network as the cathode and a lithium metal as the anode were assembled in a glove box. The mean charge and discharge voltages were around 2.7 and 3.8 V, respectively. The electrolytes were prepared with a solvent content of 50 wt % and a film thickness of around 0.1 mm. Twenty-four cycles of charging and discharging of the polymer cell that contained the gel PAN electrolyte without α-Al_2O_3 (F6A0) took 20,000 s. In contrast, when the polymer electrolyte (F6A3P50) contained only 3 wt % α-Al_2O_3, the number of cycles over the same period was 12; at 7 wt % (F6A7P50), the number of cycles was 11. Therefore, adding α-Al_2O_3 to the gel PAN electrolyte significantly improved the recharge/discharge performance. The capacity of the cells followed the order, F6A0 < F6A3P50 < F6A7P50. The capacities

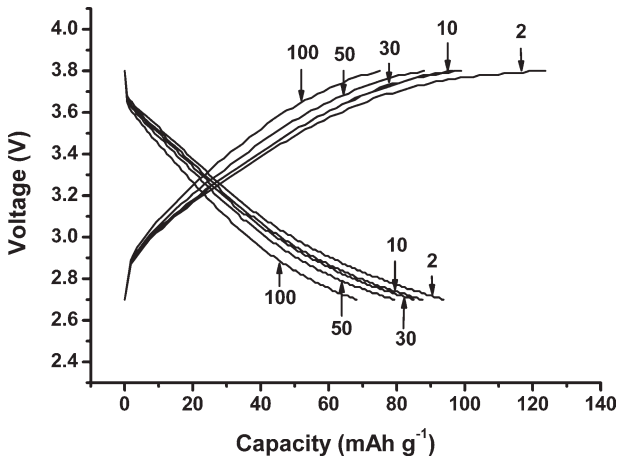

Figure 9 Charge/discharge profiles of the lithium polymer cells incorporating the gel PAN/α-Al_2O_3 nanocomposite electrolyte filled with 7 wt % α-Al_2O_3 (50 nm; F6A7P50) after 2–100 cycles.

of the electrolytes that contained α-Al_2O_3 clearly exceeded that of the electrolyte without α-Al_2O_3. Figure 9 displays the discharge and charge profiles of the lithium polymer cells that were prepared with the gel PAN/α-Al_2O_3 nanocomposite electrolyte that incorporated 7 wt % α-Al_2O_3 (50 nm; F6A7P50). The specific capacity of the cell was high (approximately 124 mA h g^{-1}) during the initial charge process; increasing the number of cycles reduced the capacity. We posit that a nonconductive substance was formed between the electrolyte and electrode, slowly increasing the interfacial resistance and reducing capacity. However, the electrolyte provided a capacity of about 93 mA h g^{-1} during the initial discharge process and a residual capacity of about 70 mA h g^{-1}, revealing high cyclability and stable capacity. The coulombic efficiency in the recharge/discharge process was about 75%, even after 100 cycles. This favorable performance is attributable to the high ionic conductivity of the electrolyte that incorporates α-Al_2O_3. These results suggest that the developed gel PAN/α-Al_2O_3 nanocomposite electrolyte system may be useful for practical battery systems.

CONCLUSIONS

Incorporating α-Al_2O_3 powder into gel PAN electrolytes transforms their properties. A series of organic/inorganic nanocomposites were obtained after α-Al_2O_3 powder was dispersed into a gel PAN electrolyte. DMA suggests that the added α-Al_2O_3 interacted noncovalently with the PAN, reducing the value of T_g of the polymeric gel electrolyte, making the polymer chain more flexible and, thereby, promoting the migration of lithium ions. The dispersion of the inorganic nanopowder into the PAN electrolyte increased not only its conductivity but also its electrochemical stability. The ionic conductivity depends on the amount and average size of the α-Al_2O_3 particles, the molar ratio of $LiClO_4$ to the PAN repeating unit [$LiClO_4/CH_2CH(CN)$], and the cosolvent content. A conductivity of around 7.48×10^{-4} S cm^{-1} was obtained at 30°C for the electrolyte with 7 wt % of 50 nm α-Al_2O_3, an F value of 0.6, a thickness of 0.10 mm, and a solvent content of 50%. The lithium/gel PAN/α-Al_2O_3 nanocomposite electrolyte/composite cell exhibited increased specific capacity and cyclability. The coulombic efficiency in the recharge/discharge process was approximately 75%, even after 100 cycles. Accordingly, the gel PAN/α-Al_2O_3 nanocomposite electrolyte seems to be appropriate for use in rechargeable lithium polymer batteries.

References

1. Besenhard, J. O. In Handbook of Battery Materials; Wiley-VCH: Weinheim, Germany, 1999; Chapter 4.
2. Armand, B.; Chabagno, J. M.; Duclot, M. J. In Fast Ion Transport in Solids; Vashista, P., Mundy, J. N., Shenoy, G. K., Eds.; Elsevier North-Holland: Amsterdam, The Netherlands, 1979; p 345.
3. Murata, K.; Izuchi, S.; Yoshihisa, Y. Electrochim Acta 2000, 45, 1501.
4. Brummer, S. B.; Koch, V. R.; In Materials for Advanced Batteries; Murphy, D.W., Broadhead, J., Steele, B. C. H., Eds.; Plenum Press: New York, 1980; p 123.
5. Dias, F. B.; Plomp, L.; Veldhuis, J. B. J. J Power Sources 2000, 88, 169.
6. Kalhammer, F. R. Solid State Ionics 2000, 135, 315.
7. Tang, Z.; Qi, L.; Gao, G. Solid State Ionics 2008, 179, 1880.
8. Baskaran, R.; Selvasekarapandian, S.; Hirankumar, G.; Bhuvanewari, M. S. J Power Sources 2004, 134, 235.
9. Okamotm, Y.; Yan, T. F.; Lee, H. S.; Skotheim, T. A. J Polym Sci Part A: Polym Chem 1993, 31, 2573.
10. Abraham, K. M. Electrochim Acta 1993, 38, 1233.
11. Alamgir, M.; Abraham, K. M. J Electrochem Soc 1993, 140, L96.
12. Nagatomo, T.; Ichikawa, C.; Omoto, O. J Electochem Soc 1987, 134, 305.
13. Tripathi, S. K.; Kumar, A.; Hashmi, S. A. Solid State Ionics 2006, 177, 2979.
14. Walkowiak, M.; Zalewska, A.; Jesionowski, T.; Waszak, D.; Czajka, B. J Power Sources 2006, 159, 449.
15. Kumar, D.; Hashmi, S. A. Solid State Ionics 2010, 181, 416.
16. Min, H. S.; Ko, J. M.; Kim, D. W. J Power Sources 2003, 119–121, 469.
17. Appetecchi, G. B.; Croce, F.; Passerini, S.; Scrosati, B.; Chem Mater 1994, 6, 538.
18. Abraham, K. M.; Alamgir, M. J Electrochem Soc 1990, 137, 1657.
19. Abraham, K. M.; Pasquariello, D. M.; Alamgir, M. J Power Sources 1993, 44, 385.
20. Kataoka, H.; Saito, Y.; Sakai, T.; Quartarone, E.; Mustarelli, P. J Phys Chem B 2000, 104, 11460.
21. Xue, R.; Huang, H.; Menetrier, M.; Chem, L. J Power Sources 1993, 44, 431.
22. Croce, F.; Gerace, F.; Dautzemberg, G.; Passerini, S.; Appetecchi, G. B.; Scrosati, B. Electrochim Acta 1994, 39, 2187.

23. Osaka, T.; Momma, T.; Ito, H.; Scrosati, B. J Power Sources 1997, 68, 392.
24. Killian, J. G.; Coffey, B. M.; Gao, F.; Poehler, T. O.; Searson, P. C. J Electrochem Soc 1996, 143, 936.
25. Vondrak, J.; Reiter, J.; Velicka, J.; Klapste, B.; Sedlarikova, M.; Dvorak, J. J Power Sources 2005, 146, 436.
26. Kim, Y. W.; Lee, W.; Choi, B. K. Electrochim Acta 2000, 45, 1473.
27. Bujdak, J.; Hackett, E.; Giannelis, E. P. Chem Mater 2000, 12, 2168.
28. Chen, H. W.; Chang, F. C. Polymer 2001, 42, 9763.
29. Capiglia, C.; Mustarelli, P.; Quartarone, E.; Tomasi, C.; Magistris, A. Solid State Ionics 1999, 118, 73.
30. Walkowiak, M.; Zalewska, A.; Jesionowski, T.; Pokora, M. J Power Sources 2007, 173, 721.
31. Sharma, J. P.; Sekhon, S. S. Solid State Ionics 2007, 178, 439.
32. Krejza, O.; Velicka, J.; Sedlarikova, M; Vondrak, J. J Power Sources 2008, 178, 778.
33. Hwang, J. J.; Liu, H. J Macromolecules 2002, 35, 7314.
34. Liu, H. J.; Hwang, J. J.; Chen-Yang, Y. W. J Polym Sci Part A: Polym Chem 2002, 40, 3873.
35. Nachao, L.; Charles, R. M.; Bruno, S. J Power Sources 240, 97–98, 240.
36. Bates, J. B.; Dudney, N. J.; Neuducker, B.; Vada, A.; Evans, C. D. Solid State Ionics 2000, 135, 33.
37. Croce, F.; Scrosati, B. J Power Sources 1993, 43, 9.
38. Borghini, M. C.; Mastragostino, M.; Passerini, S.; Scrosati, B. J Electrochem Soc 1995, 142, 2118.
39. Lee, K. H.; Lee, Y. G. Solid State Ionics 2000, 133, 257.
40. Stallworth, P. E.; Li, J.; Greenbaum, S. G.; Croce, F.; Slane, S. Solid State Ionics 1994, 73, 119.
41. Stallworth, P. E.; Li, J.; Greenbaum, S. G.; Croce, F.; Slane, S.; Salomon, M. Electrochim Acta 1995, 40, 2137.
42. Krawiec, W.; Scanlon, L. G., Jr.; Fellner, J. P.; Vaia, R. A.; Vasudevan, S.; Giannelis, E. P. J Power Sources 195, 54, 310.
43. Chen-Yang, Y. W.; Chen, H. C.; Lin, F. L.; Chen, C. C. Solid State Ionics 2002, 150, 327.